Visualisation of macropinosome maturation by the recruitment of sorting nexins

Markus C. Kerr[1], Margaret R. Lindsay[1], Robert Luetterforst[1], Nicholas Hamilton[1], Fiona Simpson[1], Robert G. Parton[1], Paul A. Gleeson[2] and Rohan D. Teasdale[1,*]

[1]Institute for Molecular Bioscience and ARC Centre in Bioinformatics, University of Queensland, St. Lucia, QLD 4072, Australia
[2]The Russell Grimwade School of Biochemistry and Molecular Biology and Bio21 Molecular Science and Biotechnology Institute, The University of Melbourne, Melbourne, VIC 3010, Australia
*Author for correspondence (e-mail: R.Teasdale@imb.uq.edu.au)

Accepted 14 July 2006
Journal of Cell Science 119, 3967-3980 Published by The Company of Biologists 2006
doi:10.1242/jcs.03167

Summary

We report that phosphoinositol-binding sorting nexin 5 (SNX5) associates with newly formed macropinosomes induced by EGF stimulation. We used the recruitment of GFP-SNX5 to macropinosomes to track their maturation. Initially, GFP-SNX5 is sequestered to discrete subdomains of the macropinosome; these subdomains are subsequently incorporated into highly dynamic, often branched, tubular structures. Time-lapse videomicroscopy revealed the highly dynamic extension of SNX5-labelled tubules and their departure from the macropinosome body to follow predefined paths towards the perinuclear region of the cell, before fusing with early endosomal acceptor membranes. The extension and departure of these tubular structures occurs rapidly over 5-10 minutes and is dependent upon intact microtubules. As the tubular structures depart from the macropinosome there is a reduction in the surface area and an increase in tension of the limiting membrane of the macropinosome. In addition to the recruitment of SNX5 to the macropinosome, Rab5, SNX1 and EEA1 are also recruited by newly formed macropinosomes, followed by the accumulation of Rab7. SNX5 forms heterodimers with SNX1 and this interaction is required for endosome association of SNX5. We propose that the departure of SNX5-positive tubules represents a rapid mechanism of recycling components from macropinosomes thereby promoting their maturation into Rab7-positive structures. Collectively these findings provide a detailed real-time characterisation of the maturation process of the macropinocytic endosome.

Supplementary material available online at
http://jcs.biologists.org/cgi/content/full/119/19/3967/DC1

Key words: Sorting nexin, Macropinosome, Maturation, Endosomal trafficking

Introduction

Despite its physiological importance and the role it plays in the invasion of a wide range of pathogens, our understanding of the molecular mechanisms involved in macropinocytosis is limited. Derived from the base of membrane ruffles in response to growth factor stimulation (Haigler et al., 1979; Shao et al., 2002), the macropinosome is a large (diameter >0.2 μm) phase-bright endocytic organelle that is readily labelled with fluid-phase markers (Swanson and Watts, 1995). In macrophages, macropinosomes mature by the progressive recruitment of late endosomal and lysosomal markers (Racoosin and Swanson, 1993). Specifically, using a fixed-cell system, Racoosin and Swanson demonstrated that 2-4 minutes after formation, macropinosomes in macrophages accumulate the late-endosome-specific small GTPase Rab7 and the lysosomal glycoprotein A. During subsequent maturation, Rab7 was lost whereas the lysosomal glycoprotein A remained at high levels (Racoosin and Swanson, 1993). Racoosin and Swanson also demonstrated that cargo such as the transferrin receptor (TfnR) was rapidly depleted from the maturing macropinosome implicating a specific membrane-sorting function during the early maturation process. Macropinosome formation is phosphoinositide 3-kinase (PI3K) dependent (Hooshmand-Rad et al., 1997), and unlike the relatively well-characterised phagosome, its regulation is receptor mediated. The mechanism of macropinosome maturation is poorly defined.

The sorting nexins (SNX) are a diverse group of hydrophilic proteins characterised by a PX domain in their N-termini that are preferentially recruited to the endosomal system by binding phosphatidylinositol 3-phosphate [PtdIns(3)*P*] and other 3-phosphoinositides (Teasdale et al., 2001). In isolation, the PX domain of SNX1 fails to localise to endosomes in vivo (Zhong et al., 2002). Zhong et al. demonstrated that this is due to the motility displayed by specific regions within the PI-binding pocket of the SNX1 PX domain (Zhong et al., 2005). They concluded that it is the obligate dimerisation of SNX1 through its long helical carboxyl domain, acting in concert with its PX domain, which generates a high-affinity 3-phosphoinositide-binding species (Zhong et al., 2005). It was subsequently revealed that the carboxyl regions of SNX1 and those of a subset of the sorting nexin family, including SNX1, SNX2, SNX4, SNX5, SNX6, SNX7, SNX8, SNX9 and SNX18 (Carlton et al., 2004), constitute a Bin/amphiphysin/Rvs (BAR) domain. The BAR domains of SNX1 and other proteins have been reported to have intrinsic membrane bending and binding

properties, distorting membranes of a given curvature into extensive elongated tubules (Carlton et al., 2004; Peter et al., 2004; Salazar et al., 2003).

Recently, we reported that unlike SNX1, which, depending on the assay used, binds PtdIns(3)*P*, PtdIns(3,5)P_2 (Cozier et al., 2002) or PtdIns(3,4,5)P_3 (Cozier et al., 2002; Zhong et al., 2002), SNX5 has the capacity to directly bind PtdIns(3)*P* and PtdIns(3,4)P_2 (Merino-Trigo et al., 2004). We also reported that SNX5 is transiently recruited to actin-rich regions of the plasma membrane in response to stimulation of the cell with epidermal growth factor (EGF) (Merino-Trigo et al., 2004). We speculated that given this shift in the subcellular distribution of SNX5 in response to EGF and the association of SNX5 with enlarged endosomal structures (Merino-Trigo et al., 2004), SNX5 might play a role in macropinocytosis.

By exploiting the association of SNX5 with macropinosomes, this study reveals the trafficking of membrane constituents from newly formed macropinosomes to the archetypal early endosome during the early stages of its maturation in real-time. Furthermore, we describe a novel interaction between SNX1 and SNX5. Using the readily microscopically resolved macropinosome as a model for endosome maturation, in conjunction with fluorescently tagged SNX5, we studied the kinetics and morphology of the macropinosome in real time using fluorescence videomicroscopy. The use of this system has provided the means to extend study of the maturation of endocytic compartments beyond the analyses of gross changes in morphology, lumenal pH and ultrastructure, usually performed in static systems, to include the dissection of transiently recruited proteins, such as the sorting nexins, to functionally discrete subdomains of the macropinosome.

Results

SNX5 associates with highly dynamic tubular extensions of the macropinosome

Previously we reported the change in membrane recruitment of SNX5 following stimulation of cells with EGF using immunofluorescence on fixed cell monolayers (Merino-Trigo et al., 2004). Following EGF treatment SNX5 was recruited to actin-rich regions of the plasma membrane and to large endosomal structures at the cell periphery. To extend these studies we have utilised real-time video imaging of live cells. The cell model system established for use in these studies was the previously described Flp-In HEK293 cell-line stably transfected with pcDNA5/FRT-EGFPSNX5, which is referred to here as HEK-GFP-SNX5 (Merino-Trigo et al., 2004). Western immunoblotting with a rabbit polyclonal antiserum specific for SNX5 indicated that the level of GFP-SNX5 protein produced was approximately two to three times that of the endogenous SNX5 (data not shown). The cells were serum-starved overnight and then exposed to 100 ng/ml of recombinant human EGF whilst being observed using an Olympus IX71 inverted fluorescence microscope.

The periphery of individual HEK-GFP-SNX5 cells was examined for two reasons. First, this is the site to which SNX5 is transiently recruited in response to EGF (Merino-Trigo et al., 2004), and second, this is the thinnest region of the cell and as such, it is ideally suited to investigation using real-time fluorescence microscopy. Fig. 1A is a montage of selected frames of a HEK-GFP-SNX5 cell that has been starved of serum overnight (see supplementary material Movie 1). At 1 minute 40 seconds, 100 ng/ml EGF was added. The total duration of the supplementary movie is 27 minutes. In this movie GFP-SNX5 was initially evident within the cytoplasm and on perinuclear puncta characteristic of endosomes. This is consistent with the current literature, which reports that SNX5 is a peripheral membrane protein that is recruited to the early endosome via its phosphoinositide-binding PX domain (Merino-Trigo et al., 2004; Teasdale et al., 2001). The addition of EGF to the media induced the plasma membrane of the cell to ruffle, before a single large (diameter >6 μm on its longest axis) irregular membrane-bound compartment heavily decorated with GFP-SNX5 was formed (asterisks). Within seconds of the formation of the compartment, GFP-SNX5 was evident on tubular structures that extended from the nascent organelle towards the perinuclear region of the cell. As time progressed, the tubular activity subsided, and with it, the recruitment of GFP-SNX5 to the newly formed compartment.

Macropinosomes are large (diameter >0.2 μm) (Swanson and Watts, 1995) phase-bright organelles that form at the base of membrane ruffles in growth-factor-stimulated cells (Haigler et al., 1979; Shao et al., 2002). They are heterogeneous in size and are readily labelled with fluid-phase markers. To verify that the structures under investigation are macropinosomes, the HEK-GFP-SNX5 cells were serum-starved overnight before being cultured in the presence of EGF, and dextran conjugated to tetramethylrhodamine (TR) for 3 minutes. The cell monolayers were then fixed in 0.9% paraformaldehyde (PFA) at 4°C before being examined using fluorescence microscopy (Fig. 1B). Dextran-TR was clearly evident within the lumen of the large compartment (diameter ≈6.8 μm) from which GFP-SNX5 tubules emanate. This observation was confirmed using real-time fluorescence videomicroscopy. Briefly, HEK-GFP-SNX5 cells were serum-starved overnight before being cultured in the presence of dextran-TR for 30 minutes; 100 ng/ml EGF was then added and the cell monolayer analysed as described in Fig. 1A in dual colour. Movie 2 in supplementary material was recorded at a frame-rate of one every 10 seconds for 5 minutes. Once again, dextran-TR was clearly evident within the lumen of a large SNX5-positive compartment and was also readily observed within tubules decorated with GFP-SNX5. Tubular structures indistinguishable from those presented here were readily observed when the parent HEK293 cell line used to generate the HEK-GFP-SNX5 cells was immunolabelled with antibodies detecting endogenous SNX1 (data not shown).

Recently, Schnatwinkel et al. described the novel PI(3)P-binding Rab5 effector, Rabankyrin 5, which, like SNX5, localises to early endosomes and macropinosomes (Schnatwinkel et al., 2004). To determine if Rabankyrin 5 is recruited to these structures, HEK293 cell monolayers were transiently co-transfected with pEYFP-Rabankyrin 5 and pCMU-myc-SNX5, serum starved, EGF treated, fixed, and examined by indirect immunofluorescence (Fig. 1C). YFP-Rabankyrin 5 and myc-SNX5 co-localised on early endosome-like structures and on larger vacuolar structures. The presence of the fluid-phase marker in the compartment, its induction with EGF, the co-localisation with Rabankyrin 5, its proximity to membrane ruffles, as well as its dimensions, confirmed that the large endosomal structures that SNX5 associated with are newly formed macropinosomes.

The ultrastructure of the compartments under investigation was further examined by electron microscopy. HEK-GFP-SNX5 cell monolayers were serum starved for 16 hours before being treated with or without 100 ng/ml EGF for 3 minutes at 37°C in medium containing 10 mg/ml HRP as a fluid-phase marker. Semi-thick plastic sections were then cut parallel to the substratum to facilitate visualisation of the complexity of the labelled compartments. HRP was evident in a variety of structures close to the plasma membrane (Fig. 2A-D). Most strikingly, HRP was observed in large structures close to the plasma membrane with the morphology and size of macropinosomes (asterisks), which were not observed in cells that were not treated with EGF. Consistent with the light microscopic data, HRP-positive tubules, presumably equivalent to those labelled with SNX5 (Fig. 1A), were seen to extend from the surface of the large structures (Fig. 2C). Quantitative analysis using immunoelectron microscopy of HEK293 cell monolayers transiently transfected with pEGFP-SNX5 revealed GFP-SNX5 labelling associated with the cytosol, the plasma membrane, on small membrane-bound structures reminiscent of endosomes and endosomal tubules, and on large electron-lucent putative macropinosomes close to the plasma membrane, shown in Fig. 2E. Quantification of untransfected HEK293 cells examined in parallel with the HEK-GFP-SNX5 cells confirmed the specificity of the immunolabelling observed (see Fig. 2 legend). The requirement for ultrathin sections and/or the specific fixation conditions needed for optimal morphology of frozen sections

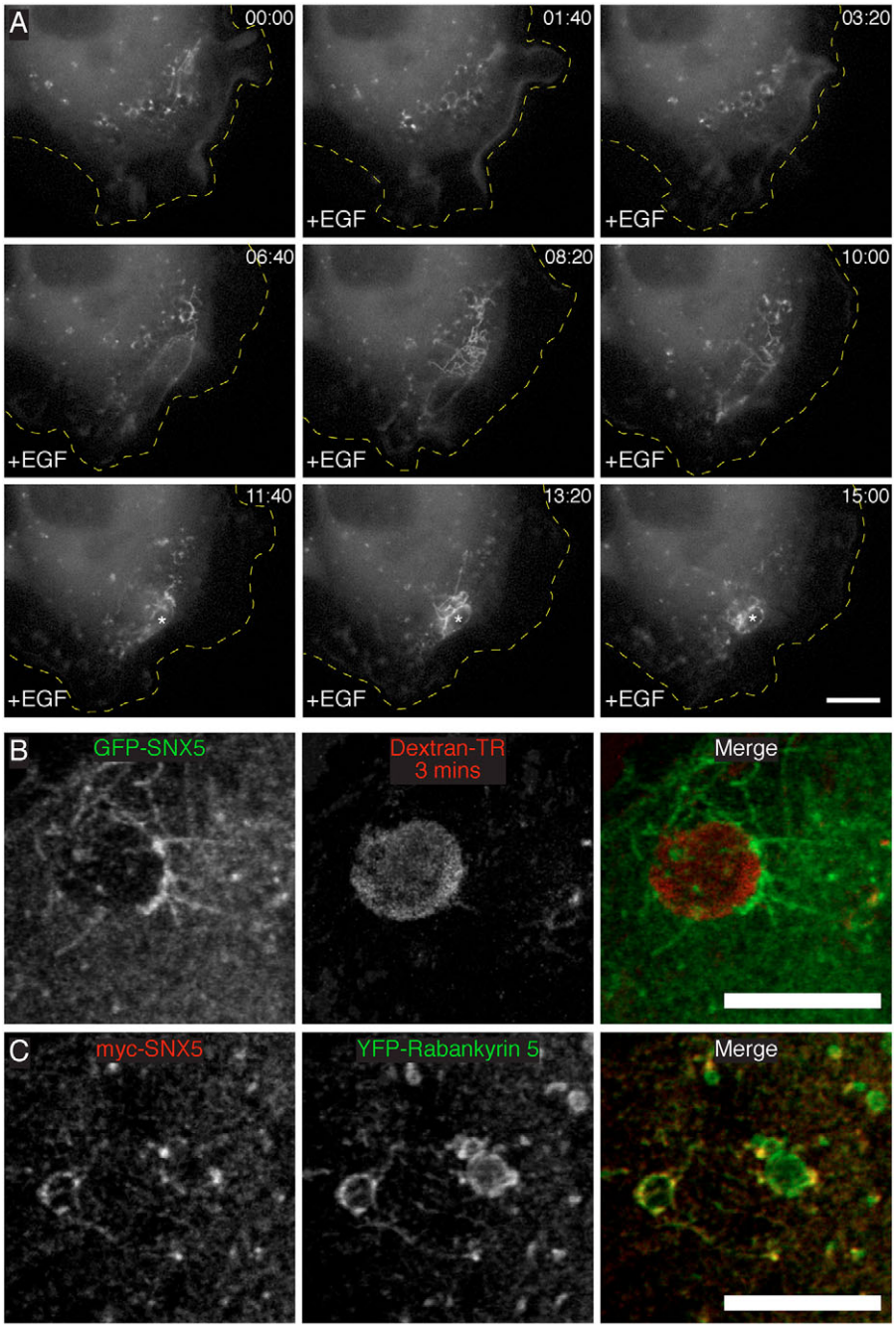

Fig. 1. EGF stimulation rapidly induces highly dynamic SNX5-positive tubule formation on newly formed macropinosomes. (A) HEK-GFP-SNX5 cell monolayers were serum starved overnight before being exposed to 100 ng/ml recombinant EGF. The interval between image capture was 10 seconds. EGF was added 1 minute and 40 seconds into the recording (+EGF). Selected frames are presented with the time captured relative to the first frame recorded at the top right (minutes:seconds). The periphery of the cell is marked in yellow. Asterisks indicate the lumen of an individual macropinosome. (B) HEK-GFP-SNX5 cell monolayers were serum starved overnight before being incubated with dextran conjugated to tetramethylrhodamine (dextran-TR) and 100 ng/ml EGF for 3 minutes before fixation with 0.9% PFA at 4°C. SNX5-positive macropinosomes were then analysed by immunofluorescence microscopy. (C) HEK293 cell monolayers were co-transfected with pEYFP-Rabankyrin 5 and pCMU-myc-SNX5 as described in the Materials and Methods, fixed with 0.9% PFA and analysed by indirect immunofluorescence using an anti-myc monoclonal antibody followed by Cy3-conjugated goat anti-mouse IgG. Bars, 10 μm.

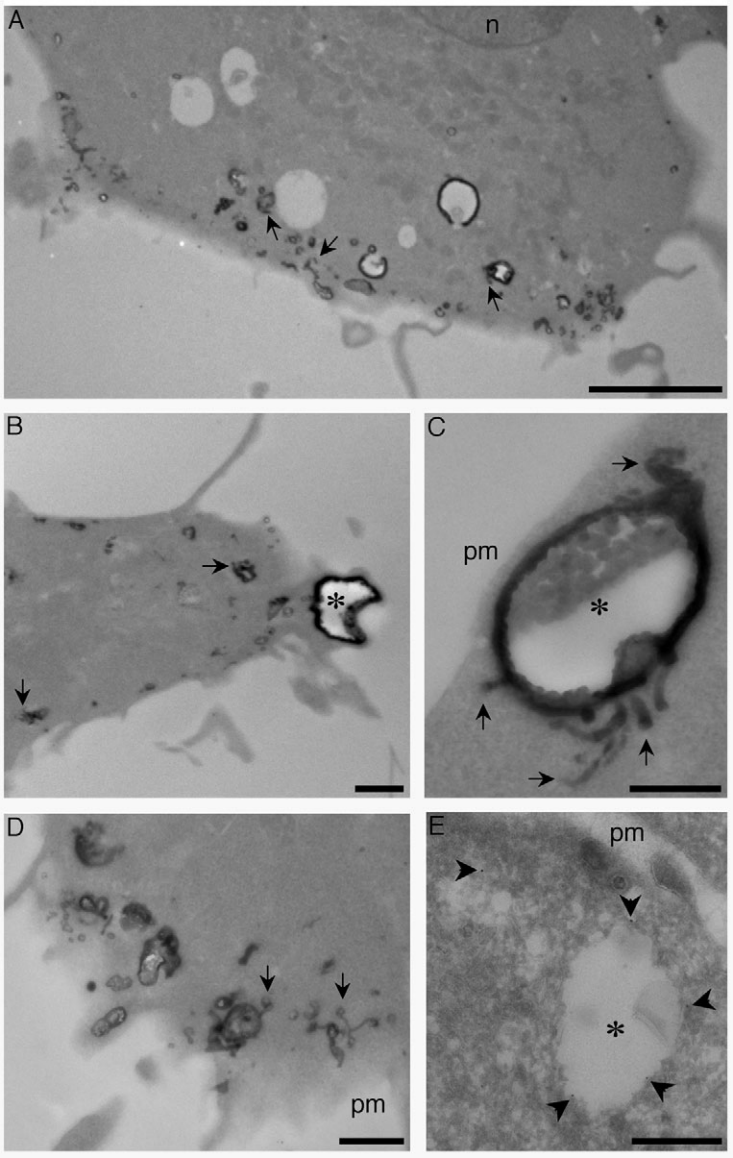

Fig. 2. Ultrastructural characterisation of growth-factor-induced pinocytic structures and localisation of SNX5 in HEK293 cells. (A-D) HEK-GFP-SNX5 cell monolayers were serum-starved overnight before being exposed to 100 ng/ml EGF and HRP for 3 minutes. The cells were then washed, fixed, and processed for plastic embedding. Semi-thick sections (200 nm) were cut parallel to the culture substratum. Asterisks indicate large HRP-labelled structures with the morphology of macropinosomes close to the plasma membrane. HRP-positive tubular structures (arrows) can be seen extending from the macropinosome-like structures. n, nucleus; pm, plasma membrane. (E) HEK293 cell monolayers were transiently transfected with pEGFP-SNX5 and serum starved overnight before being exposed to 100 ng/ml EGF for 2 minutes, fixed in 4% PFA and then processed for frozen sectioning. SNX5 in thawed sections was detected with a rabbit anti-GFP antibody followed by Protein A 10 nm gold. GFP-SNX5 labelling (arrowheads) was readily observed in the cytoplasm and on large electron-lucent vesicular structures underlying the plasma membrane. The specificity of GFP-SNX5 immunogold labelling was determined by examining random areas from 25 transfected cells and 25 untransfected cells at a magnification of 30,000×. The total number of gold particles and the number of gold particles associated with specific cellular features were compared with untransfected cells labelled in parallel under identical conditions. Total number of cytoplasmic gold particles in transfected cells is 242 and in untransfected cells is 27. The gold particle distribution was as follows (expressed as a % of total cellular labelling in transfected cells with the expected proportion contributed from background as determined from observed immunolabelling of untransfected cells in parentheses); plasma membrane, 12.0% (0%); cytosol, 67.4% (9.9%); electron-lucent vacuoles (putative macropinosomes, E), 4.1% (0%); associated tubules and small vesicles, 13.6% (0%); multivesicular bodies, 1.2% (0%); other, 1.7% (1.2%). Bars, 5 μm (A); 1 μm (B,D); 500 nm (C,E).

did not allow ready visualisation of macropinosome-associated tubular staining for SNX5. The association of GFP-SNX5 labelling within the cytosol, on the plasma membrane, and small endosome-like structures was consistent with our previous localisation studies using light microscopy (Merino-Trigo et al., 2004).

To investigate the effect of the SNX5-positive tubules on macropinosome morphology, movies were made of cells ~1 minute after EGF stimulation, when SNX5-positive tubule activity was at its greatest. Fig. 3 is a montage of selected frames taken at 10-second intervals of a single macropinosome displaying extensive SNX5-positive tubule formation and extension (see supplementary material Movie 3). Concurrent with the extension and departure of the tubular structures was a marked decrease in the diameter of the lumen of the macropinosome, suggesting that a proportion of the vacuole membrane and lumen was removed by the tubules. In addition, the morphology of the macropinosome became more circular as the time course progressed, suggesting an increase in the turgidity of the membrane. It was apparent that following the dramatic tubulation events seen in the first 5 minutes following EGF stimulation there was a marked decrease in the recruitment of GFP-SNX5 to the macropinosome, and a concomitant reduction in the rate at which SNX5-positive tubules were formed. Furthermore, the rate at which the compartment condenses slowed in accordance with the reduction in SNX5-positive tubule activity. The movie presented in this figure is representative of others taken, however, a range of phenotypes was observed, from linear tubular events to highly branched tubular structures such as those presented in Fig. 3.

Tubule extension and departure is dependent on microtubules

The majority of SNX5-positive tubular structures observed tended to be moving away from the cell periphery towards the perinuclear region of the cell. It is well established that phagolysosome maturation and the centripetal motility of

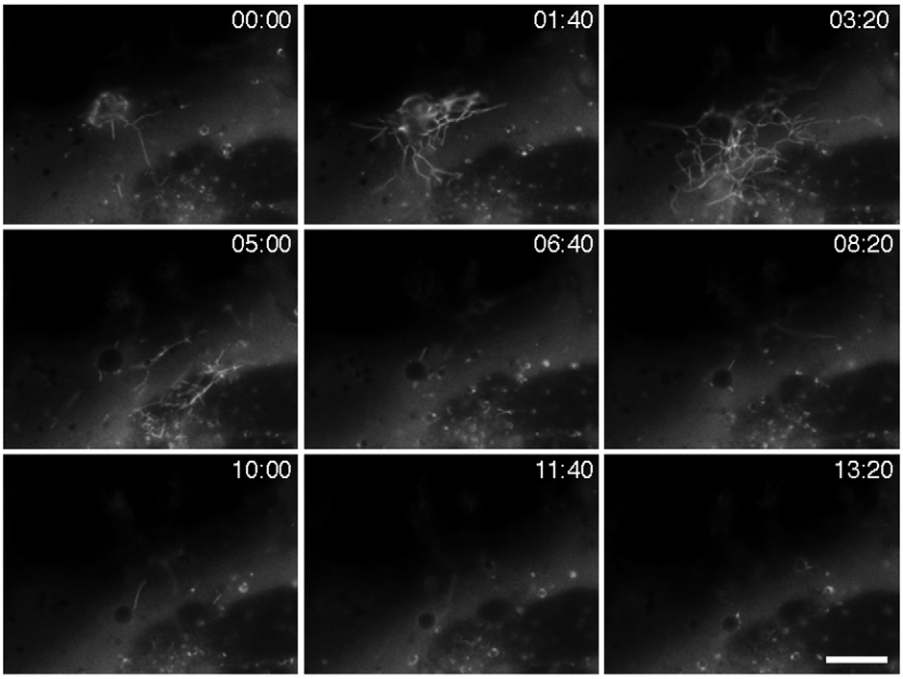

Fig. 3. SNX5-positive tubule extension and departure plays a role in the maturation of the macropinosome. HEK-GFP-SNX5 cell monolayers were serum starved overnight before being exposed to 100 ng/ml recombinant EGF ~1 minute before the videomicroscopy was started. Time-lapse movies were recorded as in Fig. 1A. The interval between image capture was 10 seconds. Selected frames are presented with the time captured relative to the first frame recorded on the top right (minutes:seconds). Bar, 10 μm.

maturing phagosomes is dependent on the microtubule network and the molecular motor dynein (Blocker et al., 1997). To determine if the SNX5-positive tubules associate with the microtubule network, HEK-GFP-SNX5 cell monolayers were serum starved overnight and treated with 100 ng/ml EGF for 5 minutes, fixed, labelled with an antibody raised against β-tubulin and examined by confocal microscopy (Fig. 4A). The SNX5-positive tubules were readily observed tracing precisely the same path as individual microtubules (arrows). To determine if the formation of these SNX5-positive tubules and their unidirectional transport was dependent upon the microtubule network, HEK-GFP-SNX5 cell monolayers were serum-starved overnight before being exposed to the microtubule-destabilising agent nocodazole (10 μM) for 30 minutes before the addition of EGF. Fig. 4B is a montage of selected frames taken at 10-second intervals of a nocodazole-treated cell following EGF stimulation (see supplementary material Movie 4). Asterisks indicate the lumen/vacuole of SNX5-positive macropinosomes. Most strikingly, although GFP-SNX5 continued to associate with macropinosomes following EGF treatment, tubule extension and departure was completely retarded. SNX5-positive tubules budded from the surface of the macropinosome, but failed to develop into elongated structures. Shortly after, formation the emergent tubules appeared to collapse back onto the cytoplasmic face of the macropinosome. This, in turn, led to retention of GFP-SNX5 on the surface of the vacuole for the full length of the time course. This differed markedly from the results presented in Fig. 1A and Fig. 3 in which the recruitment of SNX5 to the macropinosome dwindled in the later stages of the time course nor did the macropinosomes condense or become more circular.

SNX5 associates with discrete microdomains on the surface of macropinosomes

To further examine the association of SNX5 with the macropinosome membrane, we repeated the videomicroscopy experiments described above using a decreased time interval between frames. Fig. 5A is a montage of selected frames of a series taken every second of a single macropinocytic event (see supplementary material Movie 5). Notably, SNX5 was initially observed as an intense fluorescent patch (arrow) on the cytoplasmic face of the macropinosome. Following formation, the SNX5 patch traversed the surface of the macropinosome towards a tubular extension. Seventy-five seconds after patch formation, the patch docked with the base of the emergent tubule before it was integrated into the SNX5-positive tubule. In addition to providing insight into the formation and movement of the patches, these videomicroscopy experiments reveal the highly dynamic and regulated nature of the tubule formation and extension. Specifically, Fig. 5A illustrates the formation and extension of two tubular structures in succession. Both were formed from the same emergent bud, and both followed an identical path subsequent to fission from the macropinosome. This led us to speculate that they function in a directed manner, following microtubule-dependent predetermined tracks through the cell. The tubules extend from the body of the macropinosome at a rate of approximately 0.5 μm/second. Following fission, the tubules move towards the perinuclear region of the cell at 1 μm/second, before docking with a small SNX5-positive (acceptor) endosome. Concurrent with the fusion of the donor tubule with the acceptor endosome was an increase in the fluorescent intensity of the acceptor endosome, consistent with fusion having taken place. The percentage of GFP-SNX5-labelled tubules that were directed towards the perinuclear region was calculated. Of 50 macropinosomes examined, 93% of tubules trafficked to the perinuclear location, indicating a retrograde transport step.

These observations become more evident when the frames from the videomicroscopy presented in Fig. 5A are viewed as a stack in three dimensions. The data from Fig. 5A were converted into individual frames and stacked on the *Z* axis

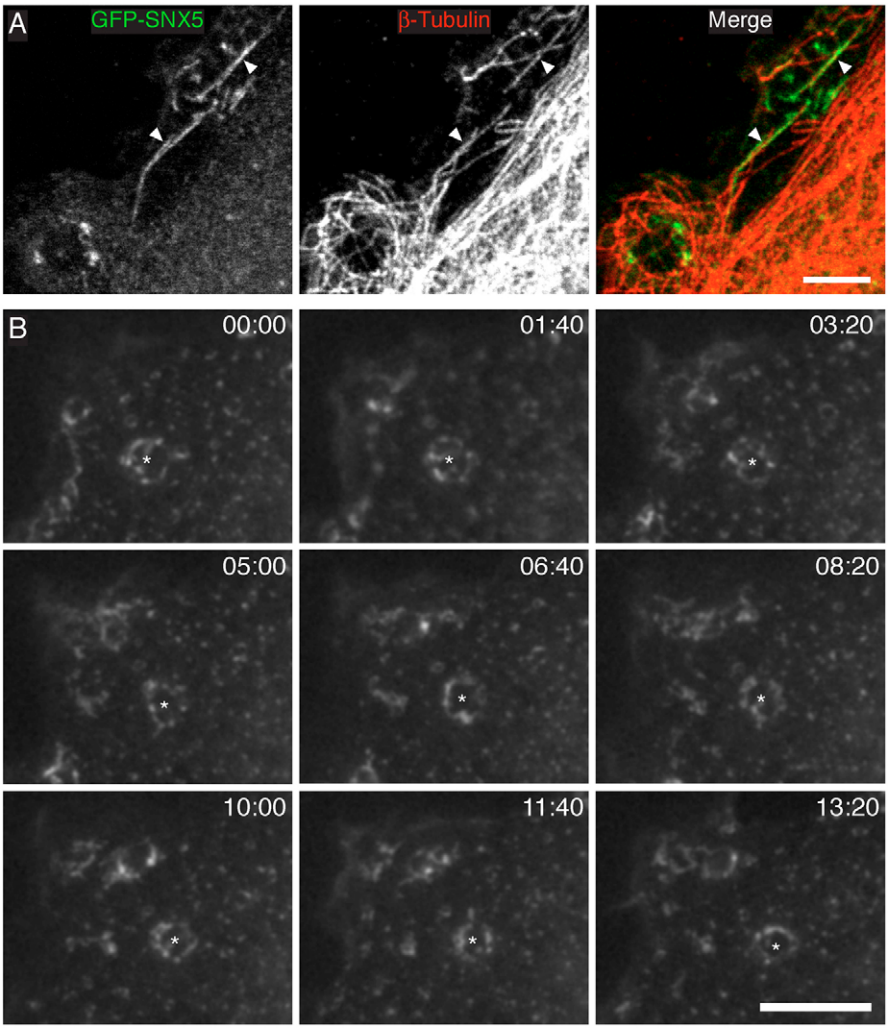

Fig. 4. Extension of SNX5-positive tubules is dependent on microtubules. (A) HEK-GFP-SNX5 cell monolayers were fixed in 0.9% PFA and analysed by indirect immunofluorescence using a monoclonal antibody against β-tubulin followed by Cy3-conjugated goat anti-mouse IgG. (B) HEK-GFP-SNX5 cell monolayers were serum starved overnight before being exposed to the microtubule-destabilising agent nocodazole (10 μM) for 30 minutes, and then to EGF as in Fig. 3. Time-lapse movies were recorded for a total period of 15 minutes with a 10-second interval between image capture. The total capture period was subsequently extended to 90 minutes with little apparent loss of fluorescent signal of GFP-SNX5 from the macropinosome. Asterisks indicate the lumen of an individual macropinosome. Bars, 5 μm (A); 10 μm (B).

using software developed for the task (F. Clark and N.H., unpublished data) (Fig. 5B). In the foreground is the first frame of the videomicroscopy experiment; in the background the last, with the intervening frames arranged between them in chronological order. As indicated (red arrows), the path tracked by the SNX5-positive patch was represented as a ridge-like projection that contorted around the macropinosome before it merged with the site of tubule activity. The acceptor endosome is evident (asterisks) as a rod-like structure, and the fusion of the donor tubule to the acceptor endosome is indicated (green arrows). This form of analysis also emphasised the path taken by the tubules as they extended towards the acceptor endosome, highlighting the conserved nature of the path taken. Movie 6 in supplementary material presents the stacked projection as it is rotated to highlight features of note.

Fluorescence compaction analyses provide the means to investigate the likelihood that two fluorescently labelled compartments have fused (Lock and Stow, 2005). To confirm that fusion between the donor tubule and acceptor endosome had occurred, the relative fluorescent intensities of the tubule and acceptor endosome, pre and post fusion were measured with Image J v1.31 and plotted against one another (Fig. 5C). These measurements revealed that the total fluorescence of the donor and acceptor membranes was equivalent to the total fluorescence of the structure post-fusion suggesting that a fusion event had occurred.

SNX5 is recruited to discrete subdomains of the macropinosome before it is incorporated into highly dynamic tubular structures (Fig. 5A-C). To emphasise the association of SNX5 with membrane microdomains of the macropinosome, 3D reconstructions were generated using optically sectioned *Z* stacks obtained with a confocal scanning laser microscope. HEK-GFP-SNX5 cell monolayers were starved of serum overnight, exposed to 100 ng/ml EGF for 5 minutes, fixed, and examined by indirect immunofluorescence. Optical sections were taken at 0.8 μm intervals, and the reconstructions generated using the LSM software (Zeiss, Germany). Fig. 6A is a single optical section of a macropinosome labelled with EEA1 and GFP-SNX5. Although SNX5 labelling was restricted to discrete portions of the macropinosome, EEA1 labelling was continuous throughout. A subset of the SNX5 subdomains was also positive for EEA1. Surface-rendered reconstructions (Fig. 6B) highlight the discrete patches of SNX5 on the cytoplasmic surface of the macropinosome.

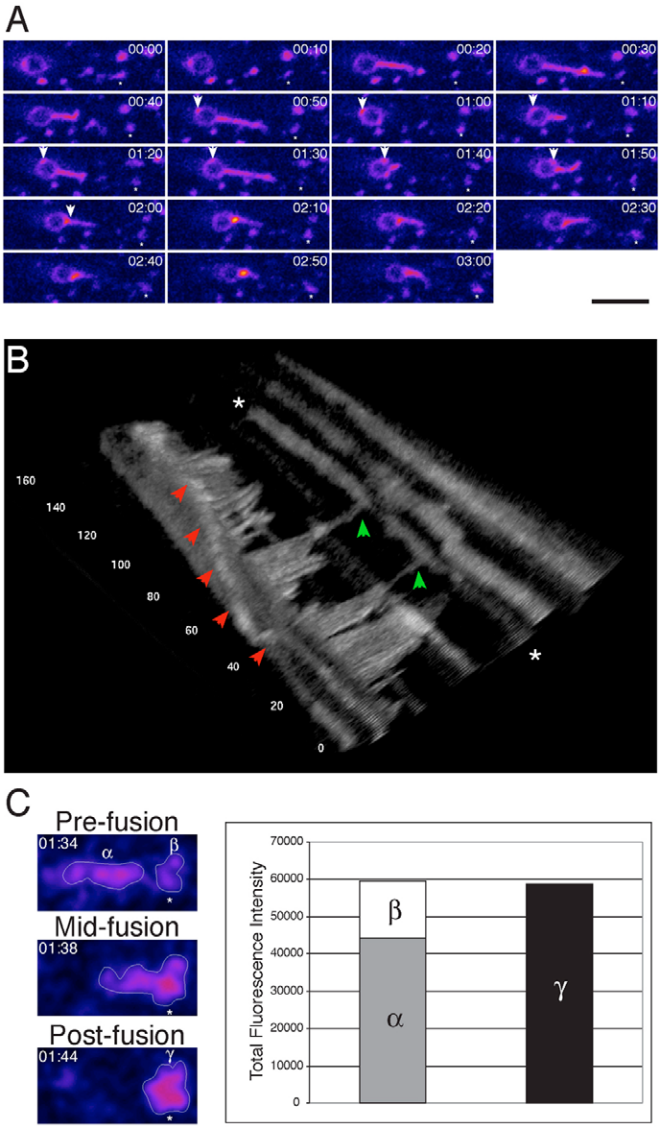

Fig. 5. Macropinosome-derived SNX5-positive tubules traffic to smaller SNX5-positive early endosomes. (A) HEK-GFP-SNX5 cell monolayers were treated and analysed using the same conditions as in Fig. 1A. The interval between images captured was 1 second for a total period of 3 minutes. Tif stacks were pseudocoloured to highlight variations in fluorescent intensity (black/blue, low intensity; white/yellow, high intensity). Arrows highlight the emergence and movement of a discrete SNX5-positive patch across the cytoplasmic face of the macropinosome. Asterisks indicate point of termination of tubules. Bar, 5 μm. (B) To visualise the kinetics of the structures presented in A, the movie was separated into individual frames using Image J v1.31 and associated Macro programs and stacked in the *Z* axis using software specifically developed for the task. The frames were arranged with the first frame in the foreground with each successive frame behind the first. Numbers in the image indicate frame numbers captured at 1-second intervals. Presented is a single view from Movie 6 in supplementary material. Red arrows highlight the path of an SNX5-positive patch across the cytoplasmic face of the macropinosome. Green arrows highlight the termination point of the tubules and asterisks indicate the acceptor endosome. (C) Fluorescent compaction was used to monitor the fusion event between the tubule and the acceptor endosome (asterisk). The relative fluorescent intensities of the tubule (α) and the acceptor endosome pre-fusion (β) and post-fusion (γ) were measured using Image Jv1.31.

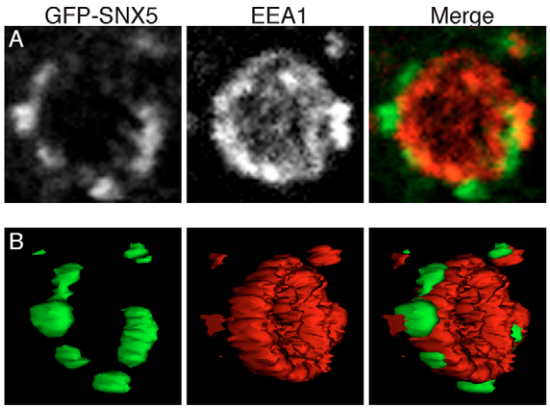

Fig. 6. SNX5 associates with discrete lipid microdomains on the surface of macropinosomes. (A) HEK-GFP-SNX5 cell monolayers were fixed in 0.9% PFA and analysed by indirect immunofluorescence using a monoclonal antibody against EEA1 followed by Cy3-conjugated goat anti-mouse IgG. (B) Surface rendered 3D reconstruction of the same macropinosome from A was generated from *Z* stacks using a LSM 510 META confocal laser-scanning microscope. Presented is a reconstruction rotated 45° on the *y*-axis. Optical sections used were 0.8 μm in depth.

SNX5-positive tubules traffic membrane from the macropinosome to the early endosome concurrent with macropinosome maturation

Given that SNX5 co-localised with the Rab5 effector, Rabankyrin 5 (Fig. 1C), we investigated the likelihood that SNX5 may co-localise with Rab5 and other markers of the endosomal pathway. HEK-GFP-SNX5 and HEK293 cell monolayers were transfected as indicated, starved overnight and treated with 100 ng/ml EGF for 5 minutes. They were then fixed with 0.9% paraformaldehyde (PFA) and SNX5 individually co-labelled with the endosome-resident proteins SNX1, EEA1, LAMP1, GFP-Rab5wt, GFP-Rab7wt and YFP-Rab11wt (Fig. 7A-F). SNX5-positive macropinosomes did not co-label with either LAMP1 or YFP-Rab11wt, which associate with late endosomes/lysosomes and recycling endosomes, respectively. The majority of SNX5-positive macropinosomes co-labelled with the early endosome markers, SNX1, GFP-Rab5wt and EEA1 and ~60% of SNX5-positive macropinosomes were GFP-Rab7wt positive. SNX1 strongly co-localised with SNX5 on both the discrete patches on the macropinosome and tubular structures. As endocytic compartments mature, a number of proteins are differentially recruited in a temporally dependent manner. Rab5 has been implicated in the formation of macropinosomes (Li et al., 1997) whereas Rab7 associates with subsequent stages of maturation and late endosomal/lysosomal fusion (Harrison et al., 2003). Interestingly, the smaller perinuclear SNX5-positive endosomal structures were also decorated with SNX1, EEA1 and GFP-Rab5wt, but not with LAMP1, GFP-Rab7wt nor with GFP-Rab11wt, suggesting that the acceptor endosomes described in Fig. 6 are traditionally defined early endosomes.

To investigate this observation in real time, HEK293 cells were transiently transfected with mCherry-SNX5 and GFP-Rab5wt or GFP-Rab7wt. Dual-colour videomicroscopy was performed as before with 2-second intervals between frames

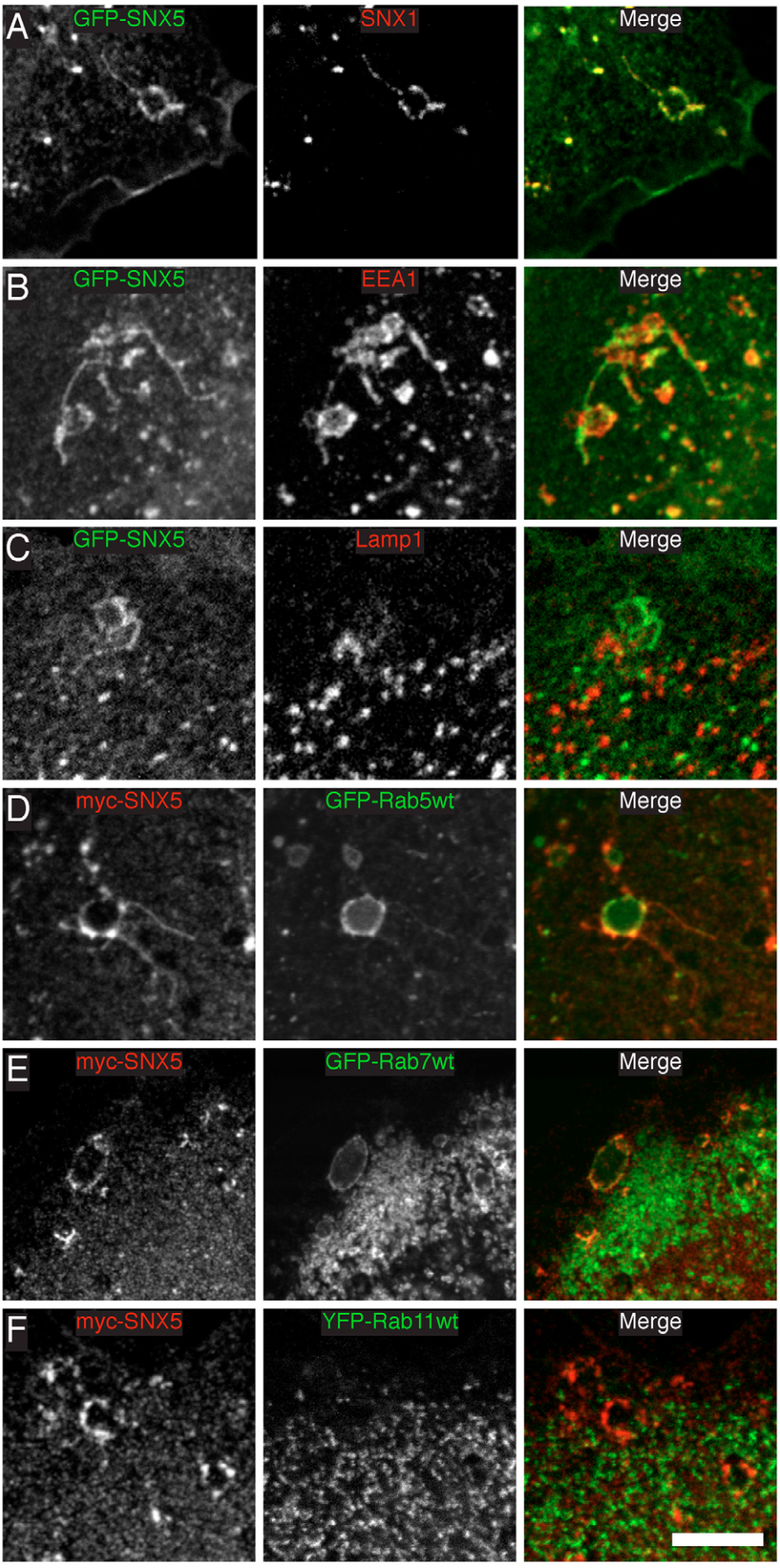

Fig. 7. SNX5 associates with early-stage macropinosomes. HEK-GFP-SNX5 and HEK293 cell monolayers were transfected as described in the Materials and Methods, serum starved overnight and exposed to 100 ng/ml EGF for 5 minutes before being fixed with 0.9% PFA. SNX5-positive macropinosomes were then analysed by indirect immunofluorescence. Images were collected as described in Fig. 1B. (A-C) HEK-GFP-SNX5 cell monolayers were labelled with monoclonal antibodies against SNX1, EEA1 and LAMP1, respectively, followed by Cy3-conjugated goat anti-mouse IgG secondary antibody. (D-F) HEK293 cell monolayers co-transfected with pCMU-myc-SNX5 and either GFP-Rab5wt (C), GFP-Rab7wt (D) or YFP-Rab11wt (E) as indicated were co-labelled with an anti-myc monoclonal antibody and Cy3-conjugated goat anti-mouse IgG. Bar, 5 μm.

(supplementary material Movies 7 and 8). Fig. 8A,B are montages of selected frames of macropinosomes co-labelled with mCherry-SNX5 and GFP-Rab5 (Fig. 8A) or mCherry-SNX5 and GFP-Rab7 (Fig. 8B) undergoing tubule formation and extension. Consistent with Fig. 3, the extension and departure of the SNX5-positive tubular structures during macropinosome maturation was associated with a marked decrease in the diameter of the lumen of the macropinosomes and an increase in their circularity. At this early stage of maturation, high levels of Rab5 were present with SNX5 on the macropinosome whereas only low levels of Rab7 are present. Furthermore, Rab5 is restricted to the body of the macropinosome and appears to be absent from the emerging tubular domains. As the macropinosome continued to mature the level of Rab7 association increased whereas the level of SNX5 decreased. The Rab5 levels were maintained or marginally decreased over this time scale.

To confirm that GFP-SNX5 is recruited to the newly formed

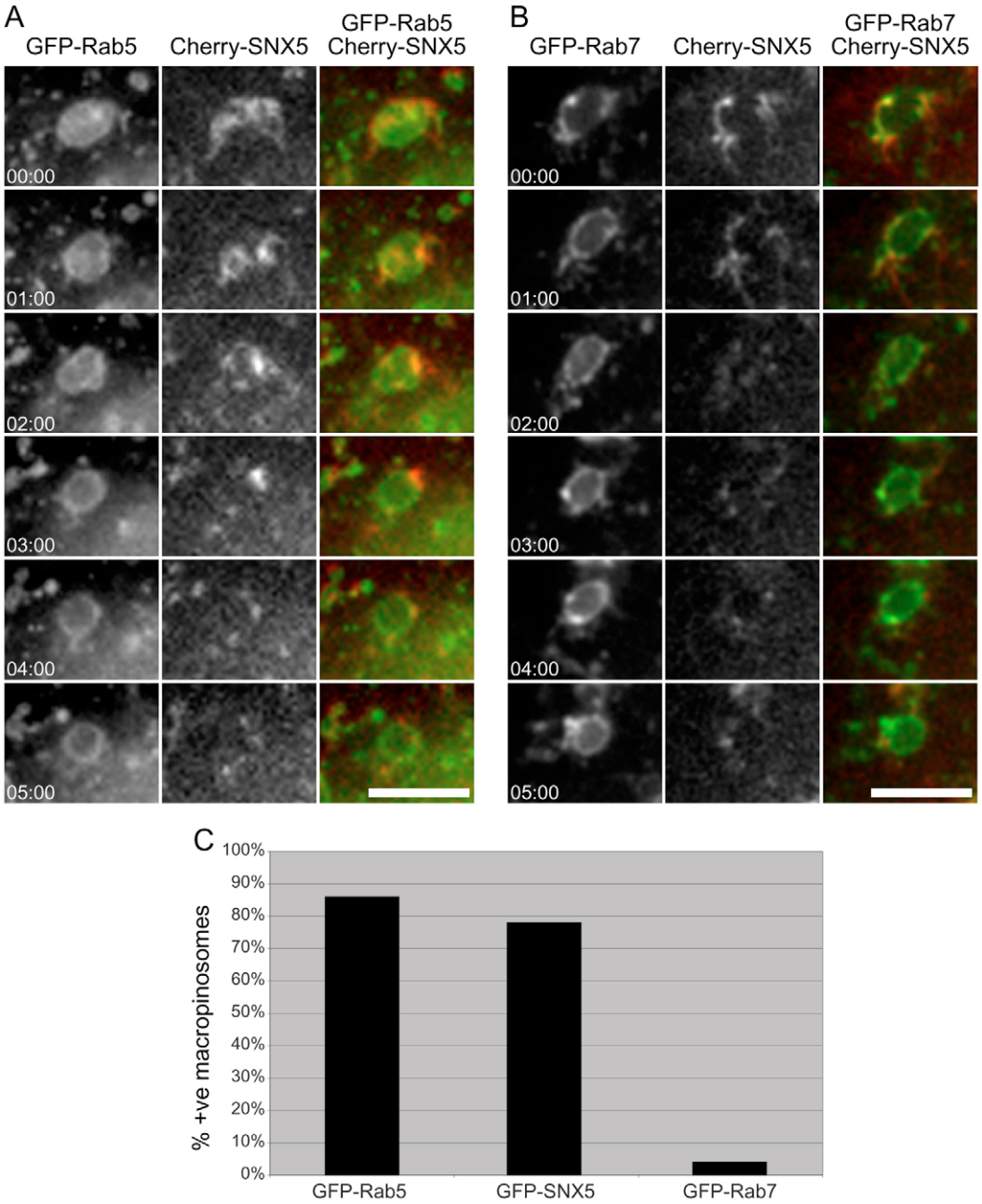

Fig. 8. SNX5-positive tubule departure is concurrent with macropinosome Rab5 to Rab7 conversion. (A,B) HEK293 cell monolayers were co-transfected with mCherry-SNX5 and either GFP-Rab5wt (A) or GFP-Rab7wt (B). Time-lapse movies were recorded with an interval between image capture of 2 seconds. Bars, 5 μm. (C) HEK-GFP-SNX5 cells and HEK293 cell monolayers transfected with either GFP-Rab5wt or GFP-Rab7wt were serum starved overnight before being incubated with dextran-TR and 100 ng/ml EGF for 3 minutes at 37°C before fixation with 0.9% PFA at 4°C. 50 dextran-positive macropinosomes (diameter >0.2 μm) were imaged and the presence of each marker was scored. Presented is the percentage of dextran-positive macropinosomes labelled with detectable levels of GFP-Rab5, GFP-SNX5 or GFP-Rab7.

macropinosome with GFP-Rab5wt and that this occurs before the recruitment of GFP-Rab7wt, HEK-GFP-SNX5 or HEK293 cells transfected with GFP-Rab5wt or GFP-Rab7wt were serum starved overnight before being incubated with dextran-TR and 100 ng/ml EGF for 3 minutes before fixation. Fifty dextran-positive macropinosomes (diameter >0.2 μm) were imaged and the presence of each protein scored as positive or negative (Fig. 8C). 86% and 78% of macropinosomes formed within 3 minutes of exposure to EGF and dextran-TR were GFP-Rab5wt- and GFP-SNX5-positive, respectively. By contrast, only 2% of newly formed macropinosomes were GFP-Rab7wt positive. The inability to detect the low levels of Rab7 as seen during the SNX5-positive stages in the live cell may reflect a loss of sensitivity when the cells were fixed. Overall, we conclude that high levels of Rab5 and SNX5 are recruited to the newly formed macropinosomes and that concurrent with the SNX5-positive tubule departure, the maturing macropinosomes recruited increasing amounts of Rab7.

Haigler and co-workers established that macropinocytosis is induced by receptor-mediated signalling events (Haigler et al., 1979; Shao et al., 2002). To examine the membrane receptors associated with the EGF induced SNX5-positive macropinosomes, cells were fixed and endocytic cargo molecules analysed by indirect immunofluorescence. Significantly, both GFP-EGFR and TfnR were present in the SNX5-positive macropinosome and smaller SNX5-positive endosomes (data not shown). However, it was unclear as to whether either of these cargo proteins are present within the SNX5-positive tubules. A difficulty in the detection of fluorescently labelled TfnR in tubules of conventional endosomes has also been noted previously (Carlton et al., 2004). Although the CI-M6PR was readily detected in the smaller SNX5-positive early endosomes, we were unable to detect CI-M6PR in the SNX5-positive macropinosome presumably as a result of relatively low levels of the receptor at the plasma membrane (data not shown).

SNX5 forms a heterodimer with SNX1 that is essential for its recruitment to endosomes

Using the yeast two-hybrid system, Haft et al. revealed that SNX1 associates with the retromer complex through a direct interaction with Vps35 (Haft et al., 2000). By contrast, other sorting nexins, including SNX2 (Haft et al., 2000) and SNX5 (Merino-Trigo et al., 2004), do not directly bind Vps35. SNX2 does, however, bind SNX1 and this is thought to be the mechanism by which it associates with the retromer complex (Haft et al., 2000). Using the same system, we have dissected the interactions that occur between SNX1 and SNX5 (Fig. 9A). No interaction between bait-SNX5 and prey-SNX5 constructs was observed, indicating that SNX5 is unable to homoligomerise. When the protocol was repeated using SNX1 as the bait, a positive reaction was observed. Similarly, when the bait and prey construct inserts were reversed a positive interaction was observed. These observations indicate that although unable to homoligomerise, SNX5 does have the capacity to heteroligomerise with SNX1. To validate these observations in vivo, co-immunoprecipitation experiments were conducted. HEK-GFP-SNX5 stable cell monolayers were lysed and immunoprecipitated using polyclonal antibodies raised against the GFP-epitope. Samples were then separated by SDS-PAGE and immunoblotted with antibodies raised against SNX1. GFP-SNX5 and SNX1 both co-precipitated as ~75 kDa (data not shown) and ~74 kDa bands, respectively (Fig. 9B).

To verify that SNX5 associates with the endosomes via the formation of SNX5:SNX1 heterodimers, we used siRNA duplexes designed to deplete SNX1 expression (Carlton et al., 2004). HEK-GFP-SNX5 cells were transfected with scrambled or SNX1-targeted siRNAs. The cells were cultured in the presence of the siRNAs for 48 hours before they were retransfected with siRNA for a further 48 hours before investigation by western immunoblotting or fixation and examination by immunofluorescence. Immunoblotting of whole-cell lysates treated with SNX1-specific duplexes for 96 hours using anti-SNX1 monoclonal antibodies confirmed that significant knockdown of endogenous amounts of SNX1 was achieved (Fig. 9C). This is in accordance with previous observations (Carlton et al., 2004). To validate the specific nature of the SNX1 depletion the samples were also immunoblotted with anti-SNX2 monoclonal antibodies. Consistent with the results of Carlton et al. (Carlton et al., 2004), no apparent affect on endogenous SNX2 was observed. Indirect immunofluorescence analysis revealed that in the majority of cells in which SNX1 was depleted to a level not detectable by immunofluorescence, GFP-SNX5 was distributed within the cytosol and not recruited to endosomes (Fig. 9D). Within the cell monolayers transfected with the scrambled siRNA control, no alteration of the GFP-SNX5 localisation was observed. Therefore, the recruitment of SNX5 to endosomal membranes is dependent upon the expression of SNX1.

Discussion

Macropinocytosis is the engulfment of large volumes of extracellular fluid at the base of membrane ruffles. It is a process fundamental to the maintenance of cellular homeostasis and is a pathway that is readily exploited by invading pathogens. Following formation, macropinosomes travel in a centripetal manner gradually contracting as they travel towards the nucleus (Swanson and Watts, 1995). Analogous to the phagolysosome, as they mature, macropinosomes acquire markers of the early and late endosome in a sequential manner before eventually fusing with the classical lysosome (Racoosin and Swanson, 1993). Despite its physiological importance, the details of macropinosome maturation are poorly defined.

Many of the proteins associated with the maturation of the early endosome/phagosome are recruited by phosphoinositide-binding FYVE and PX-domains. The sorting nexins are a diverse group of hydrophilic proteins characterised by a PX-domain in their N-termini. Previously we have reported that the stimulation of cells with EGF results in the transient recruitment of SNX5, but not SNX1, to the plasma membrane. This is possibly mediated by the capacity of SNX5 to bind PtdIns(3,4)P_2, a phosphoinositide for which SNX1 displays no affinity (Merino-Trigo et al., 2004). Indeed co-expression of mCherry-SNX5 with the PtdIns(3,4)P_2-specific probe, GFP-PH-TAPP1 (Dowler et al., 2000), revealed substantial co-localisation between the two at the plasma membrane (our unpublished observation). In this study, we demonstrate for the first time that shortly after EGF treatment, SNX5 and SNX1

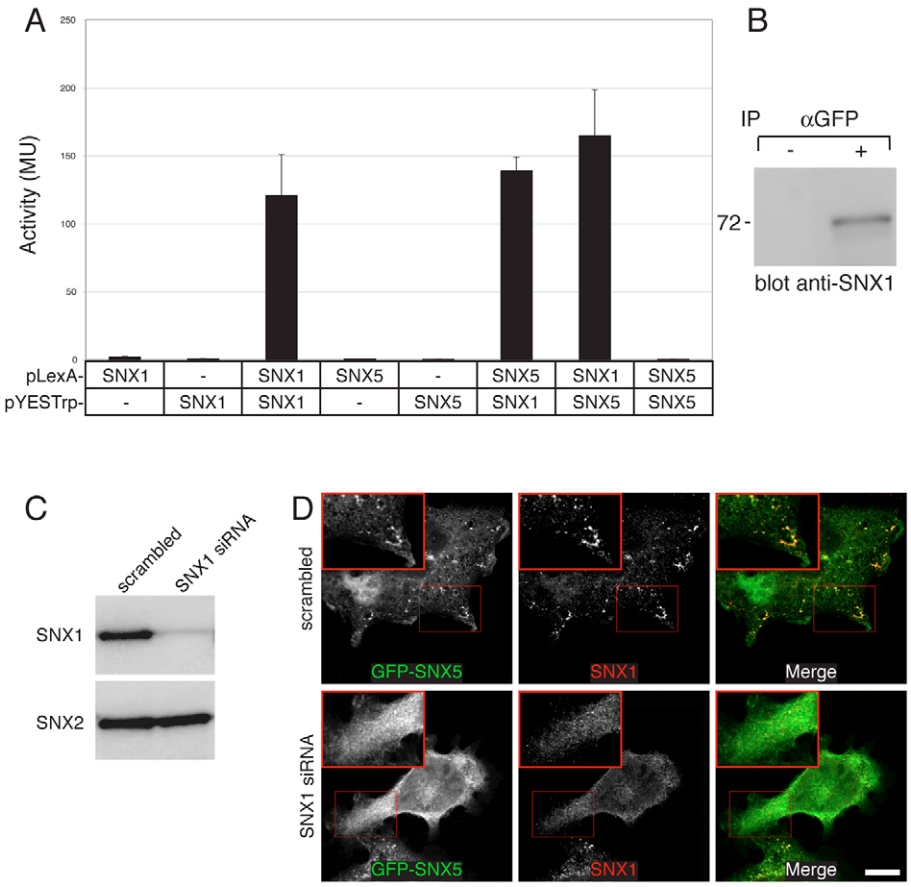

Fig. 9. SNX5 forms heteroligomers with SNX1. (A) Full-length SNX1 and SNX5 were fused to either the LexA DNA-binding domain in the pLexA vector or the B42 activation domain in the pYESTrp vector as indicated. Interactions were assessed using a liquid galactosidase assay and reported in Miller units (MU). Values are mean ± s.e.m. (B) Total extracts of HEK-GFP-SNX5 cell monolayers were prepared as described in the Materials and Methods, and lysates immunoprecipitated with an anti-GFP polyclonal antibody. Immune complexes were collected and subjected to SDS-PAGE under reducing conditions. After transfer to PVDF membranes, membranes were immunoblotted with monoclonal antibodies raised against SNX1 and HRP-conjugated anti-mouse immunoglobulin using a chemiluminescence detection system. Molecular mass in kDa is indicated on the left. (C) Total extracts of HEK-GFP-SNX5 cells treated with scrambled or *SNX1*-specific siRNA duplexes for 96 hours were prepared as described in the Materials and Methods and separated by SDS-PAGE. The relative amount of endogenous SNX1 and SNX2 in the samples was then determined by western immunoblotting with monoclonal anti-SNX1 and SNX2 antibodies. (D) HEK-GFP-SNX5 cell monolayers treated with scrambled or SNX1-specific siRNA duplexes for 96 hours were fixed in 0.9% PFA and labelled with a mouse anti-SNX1 monoclonal antibody followed by Cy3-conjugated goat anti-mouse IgG. Bar, 10 μm.

are recruited to discrete subdomains on the cytoplasmic face of the macropinosome in a manner reminiscent of the mosaic nature of the early endosome (Sönnichsen et al., 2000). These subdomains are subsequently incorporated into highly dynamic tubular structures that traffic to smaller early endosomes and whose departure is correlated with the early stages of macropinosome maturation. Finally, we define the molecular interactions between SNX5 and SNX1. The use of fluorescence videomicroscopy also provides the means to characterise the kinetics and recruitment of proteins to the macropinosome in a temporally dependent manner thereby extending our understanding of this process beyond that possible from the static systems previously studied (Racoosin and Swanson, 1993).

The recruitment of SNX5 to the macropinosome and its involvement in tubule formation and extension is highly dynamic and transient. Approximately 5-10 minutes following EGF treatment, SNX5-positive tubules have formed, extended and departed from the surface of the macropinosome. Subsequent SNX5-positive tubule formation from the macropinosome is limited. The limitation of subsequent SNX5 recruitment to the macropinosome is probably a reflection of the reduced availability of binding sites, presumably 3-phosphoinositides or cargo, rather than depletion of SNX5, because an excess of SNX5 is clearly evident in the cytoplasm. In addition, the departure of the tubules, which have a high surface area to volume ratio, results in a reduction in the surface area of the macropinosome with little loss of volume. This will, in turn, increase the internal pressure of the vacuole thereby increasing the tension or turgidity on the macropinosome membrane, limiting its capacity to deform into tubular structures. The circularity of a vacuole is indicative of the internal pressure relative to the external pressure on the cytoplasmic face of the membrane. As the tubules depart, the macropinosome becomes increasingly circular, eventually becoming a perfect circle, indicating high internal pressure. We

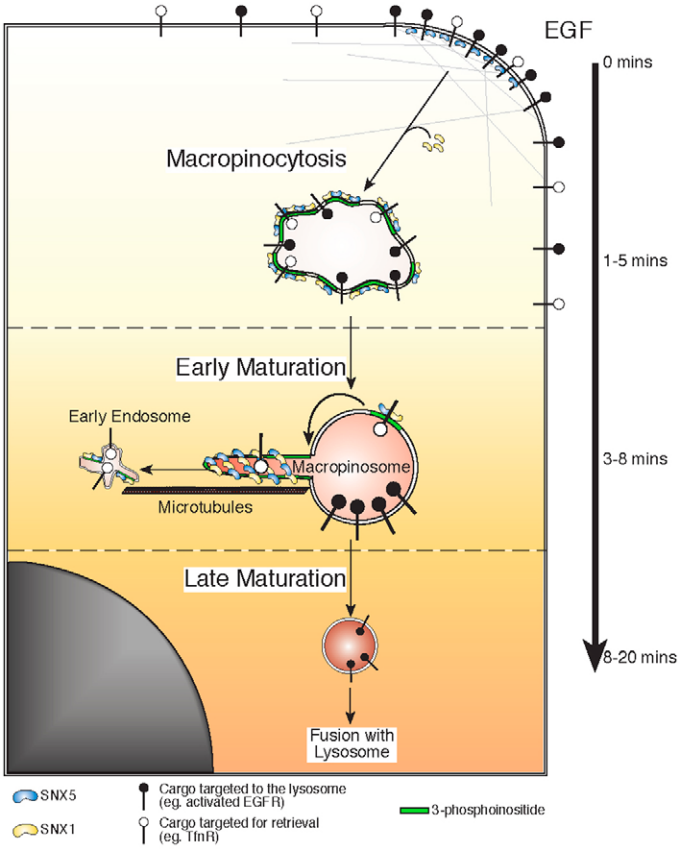

Fig. 10. Sorting nexins in macropinosome maturation. Macropinosomes are formed at the base of actin-rich membrane ruffles in response to extracellular stimuli (EGF). The sorting nexins are rapidly recruited to discrete microdomains on the nascent organelle within the first few minutes following its formation. These microdomains traverse the surface of the macropinosome in a regulated and directed manner before being incorporated into highly dynamic tubular structures. The SNX-positive tubular structures extend from the macropinosome in a microtubule-dependent fashion eventually separating from the macropinosome and travelling along predefined paths towards the perinuclear region of the cell before fusing with acceptor early endosomes. Concurrent with the departure of the tubular structure is an increase in the apparent internal pressure of the donor macropinosome as well as a shift in its protein composition.

therefore speculate that it is probably a combination of the reduction in 3-phosphoinositide availability and increased internal pressure that regulates tubule formation on macropinosomes during their early maturation phase.

The use of higher-frame-rate fluorescence videomicroscopy revealed the coordinated and regulated manner in which the SNX5-positive tubules form and extend from the macropinosome. Specifically, multiple tubules appeared to extend from the same point on the macropinosome leading us to speculate that this may be the site at which the macropinosome interacts with the cytoskeletal network. Furthermore, the emergent tubules appeared to trace the same precise path towards a small perinuclear SNX5-positive structure suggesting that they followed predefined tracks through the cell. Immunofluorescence analysis revealed that the smaller SNX5-positive compartment was readily labelled with GFP-Rab5wt, YFP-Rabankyrin 5, EEA1, GFP-EGFR, TfnR, CI-M6PR and SNX1 indicating that it is a traditional early endosome and that the SNX5-positive tubules play a role in macropinosome to early endosome trafficking.

The role of the microtubule network in centripetal and centrifugal endosomal movement is well established (Nielsen et al., 1999). Using the microtubule-destabilising agent, nocodazole (Moisoi et al., 2002), we demonstrate that the extension and subsequent fission of the SNX5-positive tubules is also dependent on the integrity of the microtubule network. In nocodazole-treated cells, SNX5-positive microdomains were observed to coalesce and emerge from the macropinosome before collapsing back onto the surface of the structure. As a consequence, unlike untreated cells, SNX5 recruitment to the macropinosome in nocodazole-treated cells is maintained for the entire time-course suggesting that the 3-phosphoinositide content of the structure is maintained. Furthermore, the macropinosomes in nocodazole-treated cells do not adopt the highly circular morphology observed in the untreated cells indicating that the internal pressure of the vacuole does not increase over time. Interestingly, these observations also suggest that the recruitment of the BAR-domain-containing sorting nexins to membranes is in itself, not sufficient to induce tubule formation in vivo. Rather, the presence of an intact microtubule network and presumably the associated microtubule-binding proteins is necessary for tubule nucleation and extension. Finally, the speed of tubule elongation, their preferential targeting towards the perinuclear region of the cell and their disruption with nocodazole is consistent with mediation by microtubule-associated motors. The most likely candidate for the role in this process is dynein (Schroer et al., 1989).

Characterisation of the resident and cargo proteins of the SNX5-positive macropinosome revealed the relatively early role SNX5 plays in macropinosome maturation. The presence of the early endosome residents EEA1 and Rab5 on SNX5-positive macropinosomes suggests that SNX5 activity is restricted to the initial stages of maturation. Furthermore, within the first three minutes of formation, intracellular dextran-positive macropinosomes simultaneously recruit SNX5 and Rab5. By contrast, at this stage they have not recruited Rab7. Therefore, the co-localisation of SNX5 with the late-endosomal resident, Rab7, on some of the macropinosomes of fixed cells represent a later stage of macropinosome maturation. This was confirmed in real time when a steady accumulation of Rab7 was observed upon the macropinosome as SNX5 was removed. This observation is consistent with those made previously, in which Rab7 was observed to accumulate upon macropinosomes 2-4 minutes post formation (Racoosin and Swanson, 1993), and places SNX5 recruitment just before that of Rab7. As co-localisation was not observed between SNX5 and the lysosome resident LAMP1, SNX5 does not appear to be associated with the macropinosome during its final stage of maturation when it fuses with the lysosome (Harrison et al., 2003).

The mosaic nature of the limiting membrane of the early endosome provides the mechanism to sort and segregate between incoming and outgoing trafficking pathways. Significantly, Sönnichsen and co-workers (Sönnichsen et al., 2000) demonstrated that endosomes are composed of discrete

subdomains, characterised by differing compositions of Rab proteins that are dynamic but do not intermix over time. These domains display properties consistent with differing functional diversities (Sönnichsen et al., 2000). The discontinuous nature of the SNX5 labelling on the macropinosome and the capacity for the sorting nexins to bind a range of selectively trafficked membrane cargo proteins indicates that SNX5 may play a role in sorting of cargo from the macropinosome to the early endosome.

Previously, we demonstrated that unlike SNX1 (Haft et al., 2000), SNX5 showed no capacity to bind directly to the core of the retromer complex, Vps35 (Merino-Trigo et al., 2004). This study reveals that SNX5 cannot homodimerise but can heterodimerise with SNX1. A SNX5 mutant analogous to the SNX1K214A mutant employed by Cozier et al. (Cozier et al., 2002), in which substitution of a conserved lysine (K214), that interacts with the 1-phosphoryl group of PI(3)P (Cozier et al., 2002), with an alanine disrupts the association of SNX1 with 3-phosphoinositides, was not recruited endosomes (unpublished observation, J. Callaghan and M.C.K). Furthermore because SNX5 is not recruited to endosomes and macropinosomes in the absence of SNX1, the recruitment of SNX5 to these membranes is dependent on its ability to form a heterodimer with SNX1 rather than simply association due to either its PX domain or BAR domain.

The use of fluorescently tagged SNX5 in HEK293 cells stimulated with EGF provides the means to observe and characterise the maturation of individual macropinosomes in real time. We have proposed a working model for the role of SNX5 in macropinosome maturation in Fig. 10. Following EGF stimulation, GFP-SNX5 is promptly recruited to discrete patches on the plasma membrane and the cytoplasmic face of newly formed Rab5- and EEA1-positive macropinosomes via its 3-phosphoinositide-binding PX domain. By forming heterodimers with SNX1, the BAR-domain of SNX5, in conjunction with that of SNX1, distorts the limiting membrane of the macropinosome into extensive tubular structures that subsequently separate from the macropinosome and traffic in a microtubule-dependent manner to perinuclear early endosomes (Rab5-, Rabankyrin 5-, EEA1-, EGFR-, TfnR- and CI-M6PR-positive). Concurrent with the departure of the tubules is a significant change in the size and morphology of the macropinosome. We propose that this trafficking pathway represents a rapid means of removing 'unwanted' components from the developing macropinosome thereby promoting its early stages of maturation into a Rab7-positive structure. For this to be the case, 'unwanted' components would need to be sorted and segregated from those targeted to the lysosome. The sorting nexins, SNX1 and SNX5, represent promising candidates for this role in the macropinosome as they have both been implicated in the sorting and trafficking of a number of different cargo proteins (Gullapalli et al., 2006; Kurten et al., 1996; Otsuki et al., 1999; Reuter et al., 2003). By using a tubular element to remove plasma membrane components rather than a spherical vesicle, the ratio of surface area to volume in the macropinosome is reduced, effectively 'tightening the slack' on the compartment. Following the 'early maturation' the developing macropinosome is then free to continue maturing before it eventually fuses with the lysosome (Racoosin and Swanson, 1993).

Materials and Methods

Antibodies, DNA constructs and reagents

Monoclonal antibodies against EEA1, LAMP1, SNX1 and SNX2 were obtained from BD Transduction Laboratories, β-tubulin was from Sigma, cation-independent mannose 6-phosphate receptor from Abcam, transferrin receptor (anti-human CD71) from Cymbus Biotechnology (Chandler's Ford, UK) and myc epitope (9B11) from Cell Signaling Technology. Polyclonal antibodies against GFP, goat anti-mouse IgG-Cy3, goat anti-rabbit IgG-Alexa-Fluor-488, and tetramethylrhodamine-dextran conjugates were purchased from Molecular Probes. Horseradish-peroxidase-conjugated anti-mouse Ig was obtained from DAKO. Recombinant human epidermal growth factor (EGF) and nocodazole were obtained from Sigma.

pEGFP-Rab5wt (Nielsen et al., 1999), pEGFP-Rab7wt (Bucci et al., 2000), pEYFP-Rab11wt (Lock and Stow, 2005), pEYFP-Rabankyrin 5 (Schnatwinkel et al., 2004) and pEGFP-EGFR (Lynch et al., 2003) were as described previously. Human transferrin receptor cloned into pCMV5 (pCMV5-TfnR) was generously provided by Prof. Volker Gerke (Institute of Medical Biochemistry, University of Münster, Germany). pCMU-myc-SNX5 was generated from a mammalian expression vector, pCMU, modified to include three repeats of the myc epitope using the same strategy as that used for the FLAG-tagged constructs described previously (Teasdale et al., 2001). pmCherry-SNX5 was generated by subcloning the full-length open reading frame of human SNX5 from GFP-SNX5 described previously (Merino-Trigo et al., 2004), into the multiple cloning site of pmCherry-C1 (Shaner et al., 2004).

Cell culture and transfection of Flp-In HEK293 cells:

HEK293 and HEK-GFP-SNX5 stable cells were generated, cultured and transfected with plasmids as described previously (Merino-Trigo et al., 2004). siRNA duplexes targeted against *SNX1* (AAGAACAAGACCAAGAGCCAC) or scrambled (AAGACAAGAACCAGAACGCCA) (Carlton et al., 2004) were supplied by Dharmacon (Lafayette, CO). Cells were transfected with 200 nM siRNA duplex while the cells were in suspension using the Hiperfect transfection reagent Fast-Forward Protocol (Qiagen) and cultured for 48 hours. Cell monolayers were subsequently retransfected and cultured for a further 48 hours.

EGF stimulation, dextran and nocodazole treatment

Cells were cultured overnight in serum-free medium before exposure to 100 ng/ml recombinant human EGF (Sigma) diluted in serum-free medium. The microtubule network of live cells was disrupted by culturing the cells in the presence of 10 μM nocodazole (Sigma) for 30 minutes. Compartments accessible to fluid-phase markers were labelled by culturing live cells in the presence of 100-200 μg/ml dextran (M_r 10,000) conjugated to tetramethylrhodamine (Molecular Probes).

Live cell imaging

Videomicroscopy was performed on individual live cells as described previously (Lock and Stow, 2005). Segments of the cell post capture were reviewed to monitor evidence of photobleaching of GFP or mCherry using the exposure times and capture intervals used in this study. Time-lapse videomicroscopy was recorded using an Olympus IX71 inverted microscope equipped with an Olympus 60× oil objective. Images were captured by an IMAGO Super VGA 12 bit 1280×1024 pixel CCD camera (TILL Photonics, Munich, Germany). Imaging control and post-capture image analysis are performed using TILLvisION software. Movies were cropped, constructed and analysed using Image J v1.31 or TILLvisION software and associated Macro programs.

3D reconstruction of real-time data

To emphasise features observed in these videomicroscopy experiments, the complete set of images was viewed as a stack in three dimensions with the first frame in the foreground. The raw images are grey scale with intensity values in the range 0 to 255. To draw out the detail from the images an intensity transfer function was applied. The intensity transfer function used was I_new(x)=255/(1+e^(k*(T–x)) where x is the original intensity and values of T=85, k=0.05 were found to give detailed clear images. The effect of the transfer function was to increase the intensity of pixels with intensity above 85, and decrease the intensity below this value. Thresholding to 0 of intensities below 60 were also applied.

Immunofluorescence assay

Cell monolayers were fixed in 0.9% or 4% (v/v) PFA and analysed by indirect immunofluorescence as described previously (Kerr et al., 2005). 3D reconstructions were generated by assembling Z stacks using the LSM 510 META software.

Electron microscopy

For Epon embedding HEK-GFP-SNX5 cell monolayers cells were serum starved for 16 hours before being cultured in warmed medium containing 10 mg/ml HRP, 0.1% BSA and 100 ng/ml EGF for 3 minutes at 37°C. Cells were placed on ice, washed in cold PBS/BSA extensively to remove surface HRP, and then fixed before DAB treatment (Parton et al., 1989) to reveal the peroxidase reaction product. Cells were then embedded in Epon and semi-thick sections of 200 nm were cut. Unstained sections were viewed using a Joel 1010 transmission electron microscope.

For cryo-electron microscopy HEK293 cell monolayers were transfected with pEGFP-SNX5, fixed in 4% PFA in 0.1 M phosphate buffer, pH 7.4 and then processed for frozen sectioning according to published methods (Liou et al., 1996). Thawed sections were labelled with rabbit anti-GFP antiserum followed by Protein A 10 nm gold. Grids were viewed using a Joel 1010 transmission electron microscope.

Yeast two-hybrid assays, immunoprecipitation and western immunoblotting

Yeast two-hybrid assays using the full-length cDNAs for human *SNX1* and *SNX5* subcloned into pLexA and pYESTrp yeast expression vectors were performed as described by Kerr et al. (Kerr et al., 2005). Immunoprecipitation of GFP-SNX5 from HEK-GFP-SNX5 cell monolayers and western immunoblotting were performed as previously described (Kerr et al., 2005).

We thank Dr Francis Clark (ACMC, UQ funded through QPSF) for software development and technical support. In addition, we thank our colleagues for providing a number of the plasmids used in this study. Confocal microscopy was performed at the ACRF/IMB Dynamic Imaging Facility for Cancer Biology, established with funding from the Australian Cancer Research Foundation. The work was supported by funds from the Australian National Health and Medical Research Council of Australia. R.D.T. is supported by an NHMRC R. Douglas Wright Career Development Award, M.C.K. was supported by an ARC Australian Post-Graduate Award, F.S. and M.R.L. are supported by UQ Fellowships. N.A.H. is supported by the award of a Federation Fellowship from the Australian Research Council to Prof. Kevin Burrage.

References

Blocker, A., Severin, F. F., Burkhardt, J. K., Bingham, J. B., Yu, H., Olivo, J. C., Schroer, T. A., Hyman, A. A. and Griffiths, G. (1997). Molecular requirements for bi-directional movement of phagosomes along microtubules. *J. Cell Biol.* **137**, 113-129.

Bucci, C., Thomsen, P., Nicoziani, P., McCarthy, J. and van Deurs, B. (2000). Rab7: a key to lysosome biogenesis. *Mol. Biol. Cell* **11**, 467-480.

Carlton, J., Bujny, M., Peter, B. J., Oorschot, V. M., Rutherford, A., Mellor, H., Klumperman, J., McMahon, H. T. and Cullen, P. J. (2004). Sorting nexin-1 mediates tubular endosome-to-TGN transport through coincidence sensing of high- curvature membranes and 3-phosphoinositides. *Curr. Biol.* **14**, 1791-1800.

Cozier, G. E., Carlton, J., McGregor, A. H., Gleeson, P. A., Teasdale, R. D., Mellor, H. and Cullen, P. J. (2002). The phox homology (PX) domain-dependent, 3-phosphoinositide-mediated association of sorting nexin-1 with an early sorting endosomal compartment is required for its ability to regulate epidermal growth factor receptor degradation. *J. Biol. Chem.* **277**, 48730-48736.

Dowler, S., Currie, R. A., Campbell, D. G., Deak, M., Kular, G., Downes, C. P. and Alessi, D. R. (2000). Identification of pleckstrin-homology-domain-containing proteins with novel phosphoinositide-binding specificities. *Biochem. J.* **351**, 19-31.

Gullapalli, A., Wolfe, B. L., Griffin, C. T., Magnuson, T. and Trejo, J. (2006). An essential role for SNX1 in lysosomal sorting of protease-activated receptor-1: evidence for retromer-, Hrs-, and Tsg101-independent functions of sorting nexins. *Mol. Biol. Cell* **17**, 1228-1238.

Haft, C. R., de la Luz Sierra, M., Bafford, R., Lesniak, M. A., Barr, V. A. and Taylor, S. I. (2000). Human orthologs of yeast vacuolar protein sorting proteins Vps26, 29, and 35, assembly into multimeric complexes. *Mol. Biol. Cell* **11**, 4105-4116.

Haigler, H. T., McKanna, J. A. and Cohen, S. (1979). Rapid stimulation of pinocytosis in human carcinoma cells A-431 by epidermal growth factor. *J. Cell Biol.* **83**, 82-90.

Harrison, R. E., Bucci, C., Vieira, O. V., Schroer, T. A. and Grinstein, S. (2003). Phagosomes fuse with late endosomes and/or lysosomes by extension of membrane protrusions along microtubules: role of Rab7 and RILP. *Mol. Cell. Biol.* **23**, 6494-6506.

Hooshmand-Rad, R., Claesson-Welsh, L., Wennstrom, S., Yokote, K., Siegbahn, A. and Heldin, C. H. (1997). Involvement of phosphatidylinositide 3′-kinase and Rac in platelet-derived growth factor-induced actin reorganization and chemotaxis. *Exp. Cell Res.* **234**, 434-441.

Kerr, M. C., Bennetts, J. S., Simpson, F., Thomas, E. C., Flegg, C., Gleeson, P. A., Wicking, C. and Teasdale, R. D. (2005). A novel mammalian retromer component, Vps26B. *Traffic* **6**, 991-1001.

Kurten, R. C., Cadena, D. L. and Gill, G. N. (1996). Enhanced degradation of EGF receptors by a sorting nexin, SNX1. *Science* **272**, 1008-1010.

Li, G., D'Souza-Schorey, C., Barbieri, M. A., Cooper, J. A. and Stahl, P. D. (1997). Uncoupling of membrane ruffling and pinocytosis during Ras signal transduction. *J. Biol. Chem.* **272**, 10337-10340.

Liou, W., Geuze, H. J. and Slot, J. W. (1996). Improving structural integrity of cryosections for immunogold labeling. *Histochem. Cell Biol.* **106**, 41-58.

Lock, J. G. and Stow, J. L. (2005). Rab11 in recycling endosomes regulates the sorting and basolateral transport of E-cadherin. *Mol. Biol. Cell* **16**, 1744-1755.

Lynch, D. K., Winata, S. C., Lyons, R. J., Hughes, W. E., Lehrbach, G. M., Wasinger, V., Corthals, G., Cordwell, S. and Daly, R. J. (2003). A Cortactin-CD2-associated protein (CD2AP) complex provides a novel link between epidermal growth factor receptor endocytosis and the actin cytoskeleton. *J. Biol. Chem.* **278**, 21805-21813.

Merino-Trigo, A., Kerr, M. C., Houghton, F., Lindberg, A., Mitchell, C., Teasdale, R. D. and Gleeson, P. A. (2004). Sorting nexin 5 is localized to a subdomain of the early endosomes and is recruited to the plasma membrane following EGF stimulation. *J. Cell Sci.* **280**, 22962-22967.

Moisoi, N., Erent, M., Whyte, S., Martin, S. and Bayley, P. M. (2002). Calmodulin-containing substructures of the centrosomal matrix released by microtubule perturbation. *J. Cell Sci.* **115**, 2367-2379.

Nielsen, E., Severin, F., Backer, J. M., Hyman, A. A. and Zerial, M. (1999). Rab5 regulates motility of early endosomes on microtubules. *Nat. Cell Biol.* **1**, 376-382.

Otsuki, T., Kajigaya, S., Ozawa, K. and Liu, J. M. (1999). SNX5, a new member of the sorting nexin family, binds to the Fanconi anemia complementation group A protein. *Biochem. Biophys. Res. Commun.* **265**, 630-635.

Parton, R. G., Prydz, K., Bomsel, M., Simons, K. and Griffiths, G. (1989). Meeting of the apical and basolateral endocytic pathways of the Madin-Darby canine kidney cell in late endosomes. *J. Cell Biol.* **109**, 3259-3272.

Peter, B. J., Kent, H. M., Mills, I. G., Vallis, Y., Butler, P. J., Evans, P. R. and McMahon, H. T. (2004). BAR domains as sensors of membrane curvature: the amphiphysin BAR structure. *Science* **303**, 495-499.

Racoosin, E. L. and Swanson, J. A. (1993). Macropinosome maturation and fusion with tubular lysosomes in macrophages. *J. Cell Biol.* **121**, 1011-1020.

Reuter, T. Y., Medhurst, A. L., Waisfisz, Q., Zhi, Y., Herterich, S., Hoehn, H., Gross, H. J., Joenje, H., Hoatlin, M. E., Mathew, C. G. et al. (2003). Yeast two-hybrid screens imply involvement of Fanconi anemia proteins in transcription regulation, cell signaling, oxidative metabolism, and cellular transport. *Exp. Cell Res.* **289**, 211-221.

Salazar, M. A., Kwiatkowski, A. V., Pellegrini, L., Cestra, G., Butler, M. H., Rossman, K. L., Serna, D. M., Sondek, J., Gertler, F. B. and De Camilli, P. (2003). Tuba, a novel protein containing bin/amphiphysin/Rvs and Dbl homology domains, links dynamin to regulation of the actin cytoskeleton. *J. Biol. Chem.* **278**, 49031-49043.

Schnatwinkel, C., Christoforidis, S., Lindsay, M. R., Uttenweiler-Joseph, S., Wilm, M., Parton, R. G. and Zerial, M. (2004). The Rab5 effector Rabankyrin-5 regulates and coordinates different endocytic mechanisms. *PLoS Biol.* **2**, E261.

Schroer, T. A., Steuer, E. R. and Sheetz, M. P. (1989). Cytoplasmic dynein is a minus end-directed motor for membranous organelles. *Cell* **24**, 937-946.

Shaner, N. C., Campbell, R. E., Steinbach, P. A., Giepmans, B. N., Palmer, A. E. and Tsien, R. Y. (2004). Improved monomeric red, orange and yellow fluorescent proteins derived from Discosoma sp. red fluorescent protein. *Nat. Biotechnol.* **22**, 1567-1572.

Shao, Y., Akmentin, W., Toledo-Aral, J. J., Rosenbaum, J., Valdez, G., Cabot, J. B., Hilbush, B. S. and Halegoua, S. (2002). Pincher, a pinocytic chaperone for nerve growth factor/TrkA signaling endosomes. *J. Cell Biol.* **157**, 679-691.

Sönnichsen, B., De Renzis, S., Nielsen, E., Rietdorf, J. and Zerial, M. (2000). Distinct membrane domains on endosomes in the recycling pathway visualized by multicolor imaging of Rab4, Rab5, and Rab11. *J. Cell Biol.* **149**, 901-914.

Swanson, J. A. and Watts, C. (1995). Macropinocytosis. *Trends Cell Biol.* **5**, 424-428.

Teasdale, R. D., Loci, D., Houghton, F., Karlsson, L. and Gleeson, P. A. (2001). A large family of endosome-localized proteins related to sorting nexin 1. *Biochem. J.* **358**, 7-16.

Zhong, Q., Lazar, C. S., Tronchere, H., Sato, T., Meerloo, T., Yeo, M., Songyang, Z., Emr, S. D. and Gill, G. N. (2002). Endosomal localization and function of sorting nexin 1. *Proc. Natl. Acad. Sci. USA* **99**, 6767-6772.

Zhong, Q., Watson, M. J., Lazar, C. S., Hounslow, A. M., Waltho, J. P. and Gill, G. N. (2005). Determinants of the endosomal localization of sorting nexin 1. *Mol. Biol. Cell* **16**, 2049-2057.